EPJ Web of Conferences **106**, 01005 (2016)
DOI: 10.1051/epjconf/201610601005

Characterization of the Annular Core Research Reactor (ACRR) Neutron Radiography System Imaging Plane

Krista Kaiser[1], K. Chantel Nowlen[2], and K. Russell DePriest[3]

[1] Senior Nuclear Reactor Engineer & Operator, Nuclear Facility Operations, Sandia National Laboratories, P.O. Box 5800, MS1142, Albuquerque, New Mexico 87185-1142, USA
[2] R&D Systems Engineer & Nuclear Reactor Operator, Nuclear Engineering and Maintenance, Sandia National Laboratories, P.O. Box 5800, MS1142, Albuquerque, New Mexico 87185-1142, USA
[3] Principal R&D Scientist & Engineer, Applied Nuclear Technologies, Sandia National Laboratories, P.O. Box 5800, MS1146, Albuquerque, New Mexico 87185-1146, USA

Abstract. The Annular Core Research Reactor (ACRR) at Sandia National Laboratories (SNL) is an epithermal pool-type research reactor licensed up to a thermal power of 2.4 MW. The ACRR facility has a neutron radiography facility that is used for imaging a wide range of items including reactor fuel and neutron generators. The ACRR neutron radiography system has four apertures (65:1, 125:1, 250:1, and 500:1) available to experimenters. The neutron flux and spectrum as well as the gamma dose rate were characterized at the imaging plane for the ACRR's neutron radiography system for the 65:1, 125:1 and 250:1 apertures.

1. Introduction

The Annular Core Research Reactor (ACRR) is located at Sandia National Laboratories (SNL) on the Kirtland Air Force Base in Albuquerque, New Mexico, USA. The ACRR has four main experimental cavities: the central cavity, the fueled ring external cavity, the neutron radiography tube and the tri-element chamber. The core consists of 236 UO_2-BeO fuel elements and 11 reactivity control rods. The neutron spectrum within the fueled region of the central cavity is epithermal. The purpose of this research was to determine the neutron spectrum and flux at the imaging plane of the neutron radiography tube. The imaging plane is located at the opening of the neutron radiography tube. The neutron radiography tube is comprised of three sections of tube with a total length of approximately 26 feet ($\sim$8 m), which is horizontally offset from the reactor core and separated by a square aluminum window, and the highest section of the tube is open at the top with a 25 inches by 25 inches (63.5 cm$\times$63.5 cm) plane available for experimental access (imaging plane). A collimator composed of alternating layers of lead, cadmium and polyurethane sits on the experimental region or base of the neutron radiography tube. The experimental region contains deuterium tanks to thermalize the epithermal spectrum of neutrons entering the neutron radiography chamber. The collimator essentially rests on the first tube section attached to the experimental region. Figure 1 displays a Solid Works rendering and a Monte Carlo

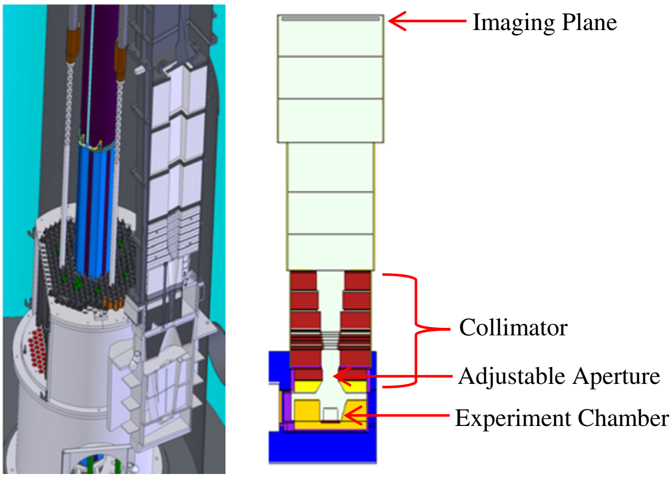

Figure 1. Solid Works and MCNP Models of the ACRR Neutron Radiography System.

N-Particle (MCNP) version 5 [1] model of the neutron radiography tube in relation to the ACRR and pictures the collimator installed. The collimator has four apertures, 65:1, 125:1, 250:1 and 500:1 which control the size of the opening in the collimator through which the radiation passes. The 500:1 aperture is currently plugged and dosimetry results were not able to be obtained and this aperture will not be included in this initial characterization work.

1.1 Materials and Methods

MCNP was used to model the neutron radiography tube to provide an estimated neutron energy spectrum, neutron flux, and gamma energy spectrum at the imaging plane (the top of the radiography tube). A neutron flux mesh tally was also modeled over the imaging plane. The KCODE card was used in MCNP to initiate source particle locations and the first 150 cycles were inactive cycles to ensure that neutron spectrum was stabilized before beginning tallies. The neutrons from the ACRR core are epithermal; the neutrons enter the neutron radiography "window" and then are attenuated by the deuterium tanks. The reduced energy neutrons then scatter 90 degrees up to the collimator region; the collimator length is approximately 8 feet ($\sim$240 cm). Once the neutrons leave the collimator there is approximately 18 feet ($\sim$550 cm) of air before reaching the imaging plane. This complicated geometry coupled with rather substantial distances between the source of the neutrons (core) and the imaging plane required the use of variance reduction techniques and parallel processing to obtain adequate statistics at the imaging plane. The MCNP files were run on 4096 computer cores for 96 hours.

Dosimetry foils and detectors were used to benchmark the MCNP model. Dysprosium (Dy) and Indium (In) were selected to be used as activation foils based upon initial MCNP results. The In dosimetry was counted using a High Purity Germanium (HPGe) detector for gamma spectrum analysis and the Dy dosimetry was counted using a gas proportional counter for the beta decay. Nickel and Sulfur activation foils were also placed on the imaging plane to confirm the lack of a fast neutron spectrum (no results are included because there was no activation of these foils). Calcium Fluoride (CaF) thermoluminescent dosimetry (TLD) was used to measure gamma dose because it provides a comparison to an electronic component rather than to tissue. This work is concerned with dose to components and not to personnel.

A 0.15 inch (0.4 cm) aluminum plate was placed over the imaging plane for the characterization work. A lattice was drawn on the aluminum plate and translucent Maslin cloth was placed over the

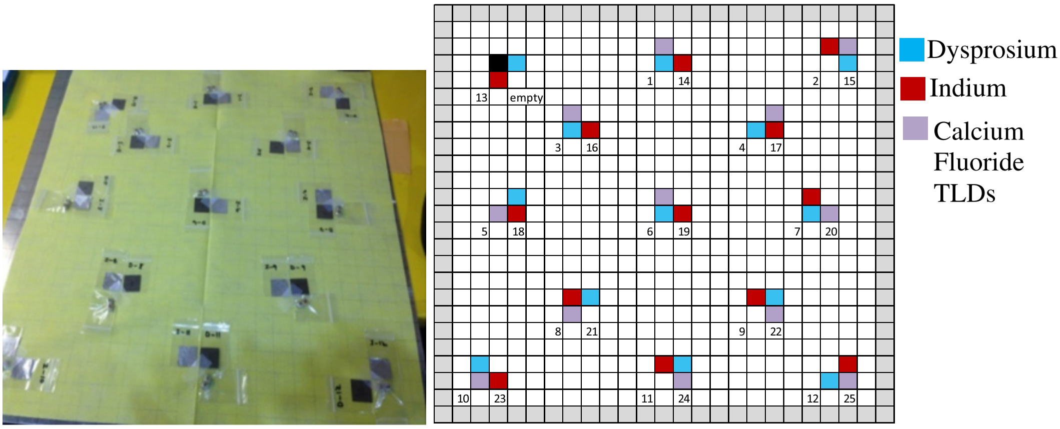

Figure 2. Aluminum Plate with Dosimetry and Corresponding Foil Pattern.

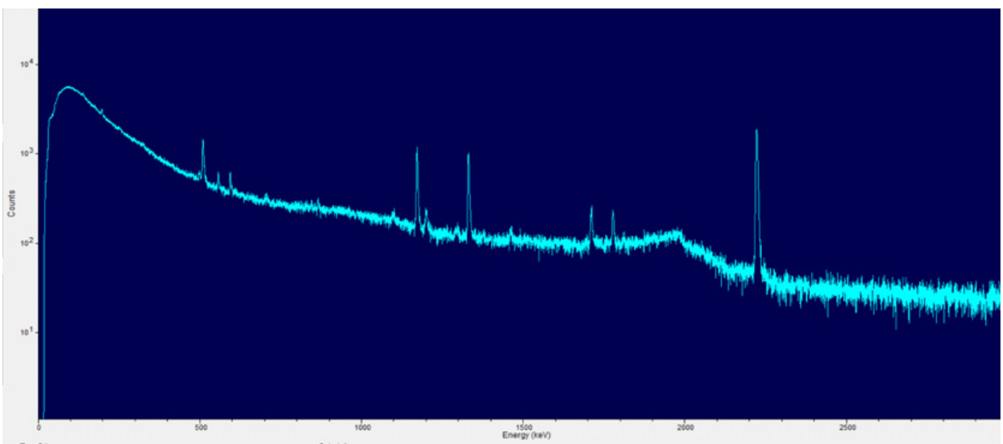

Figure 3. HPGe Gamma Spectrum.

plate. The dosimetry foils were placed in individual plastic zip bags to minimize contamination spread while handling the foils post-irradiation. The foils/bags were taped to the Maslin cloth to prevent the movement of foils during irradiation. The Maslin cloth also simplified removal of the foils post-irradiation to minimize personnel dose from the activated aluminum plate. Figure 2 provides a photo of the imaging plate setup with the foils in a specified arrangement as defined by the adjacent diagram, with the numbers indicating the foil identifiers in two sets.

With the assistance of health physics personnel [2], a Neutron MicroSpec was used to determine a neutron energy spectrum and to quantify the neutron counts at the imaging plane. The Neutron MicroSpec confirmed a thermal spectrum with all counts less than 10 keV. The lowest energy bin of the Neutron Micro Spec was from 0 to 10 keV and all interactions were within this bin. Due to the high dead time of the detector at a minimal reactor power level, further specificity in neutron spectrum was not possible. In addition, a portable High Purity Germanium (HPGe) detector provided a gamma spectrum at the imaging plane. Figure 3 displays the HPGe gamma spectrum at the imaging plane, displaying counts versus energies from 0–3000 keV. A peak search was not conducted due to the significant gamma attenuation through the collimator and subsequent peak shift.

Table 1. Tally Multipliers for Calculating Flux.

Factor	**Value**	**Unit**
F4 Tally	x (from results)	1/cm^2
Power	2.16 (*90*)	MW (*% Reactor Power*)
υ (Nu)	2.44	Neutrons/fission (average)
k_{eff}	1.0548	
Energy per fission	198	MeV/fission
Tally to Flux Conversion Factor	1.575×10^{17}	n/s

2. Results

For the MCNP modeling, to improve the statistics due to the low number of particles reaching the imaging plane, a total of 15,500 KCODE cycles were run for each aperture, with 150 inactive cycles and with the 250:1 aperture terminating early at 14,696 cycles due to an issue with the multiprocessor.

The dosimetry foils and TLDs were irradiated at 90% reactor power for 15, 30 and 45 minutes for the 65:1, 125:1 and 250:1 apertures respectively due to the variation in size of the apertures. Estimation of the time required for each aperture was calculated based off local dose rates measured when operating each aperture and assuming a linear relation between dose rate and flux.

2.1 Neutron Flux Maps

Spatial neutron flux maps were created in MCNP for each of the apertures using a mesh tally which calculated the total neutron flux at each grid location of the imaging plane and at all energies (the mesh tally energy bounds were left as default). Neutron and photon tallies were also taken in energy bins over the same area to model the neutron and gamma energy spectrum.

The numerical output from MCNP are for an F4 tally, or a track length estimate of cell flux over the volume of each mesh region, with units of cm^{-2} rather than flux; Table 1 provides the multiplying factors to obtain flux based on the desired reactor power level [3].

The flux at each location was then arranged in a map to reflect its physical orientation for analysis. The coordinates along the edge in grey indicate the center of each grid location, in cm, with the center of the grid at (0, 0). The flux maps for the three apertures tested experimentally are shown below (Figs. 4, 5 and 6).

The error associated with the 65:1 and 125:1 apertures are near 10% which are generally reliable, but the results for the 250:1 aperture were so high that they are included here for comparison, but clearly from the non-regular distribution, cannot be considered accurate.

2.2 Neutron Flux Calculation Based on Dosimetry

The results of the gamma spectrum analysis on the dosimetry foils [4] were given in specific activity in Bq/g, which was used to calculate flux using neutron activation analysis per Eq. (1) [5].

$$\Phi = \frac{A_s * \mathrm{mass}_i * \exp(\lambda * t_d)}{N * \sigma * [1 - \exp(-\lambda * t_{irr})] * (1 - \exp(-\lambda * t_c))} \tag{1}$$

where A_s is the specific activity in Bq/g at the end of the counting period, N is the number of atoms in the sample, σ is the microscopic cross section of the isotope in cm^2, λ is the isotopic decay constant in s^{-1}, t_{irr} is the time the sample was irradiated (in seconds), t_d was the decay time (in seconds) or the time between when the sample was finished being irradiated until the time that the sample count began, and t_c is the time the sample was counted (in seconds) and mass is the isotopic mass in grams. The specific activity results included the detector efficiency.

1	25.2	3.38E+06	5.36E+06	4.70E+06	6.74E+06	6.43E+06	7.24E+06	6.41E+06	6.81E+06	5.28E+06	4.84E+06
2	19.6	5.32E+06	6.89E+06	7.34E+06	7.88E+06	9.37E+06	9.88E+06	8.66E+06	8.37E+06	8.98E+06	7.12E+06
3	14	4.68E+06	7.47E+06	8.20E+06	8.61E+06	9.00E+06	1.06E+07	9.05E+06	8.40E+06	1.00E+07	6.65E+06
4	8.4	5.14E+06	8.40E+06	9.68E+06	9.21E+06	9.29E+06	9.93E+06	9.87E+06	1.07E+07	8.78E+06	8.37E+06
5	2.8	5.85E+06	7.39E+06	8.69E+06	9.41E+06	1.08E+07	9.47E+06	1.05E+07	8.83E+06	9.36E+06	8.36E+06
6	-2.8	5.94E+06	7.34E+06	9.71E+06	8.74E+06	1.08E+07	1.04E+07	9.25E+06	8.88E+06	9.55E+06	7.23E+06
7	-8.4	4.71E+06	6.50E+06	8.89E+06	9.00E+06	1.12E+07	9.37E+06	9.76E+06	9.23E+06	8.34E+06	6.15E+06
8	-14	5.13E+06	6.78E+06	8.14E+06	8.26E+06	9.89E+06	8.51E+06	8.66E+06	8.75E+06	8.58E+06	7.53E+06
9	-19.6	4.71E+06	5.72E+06	6.83E+06	8.15E+06	7.65E+06	7.41E+06	8.66E+06	8.94E+06	8.51E+06	5.61E+06
10	-25.2	3.36E+06	4.66E+06	6.06E+06	7.07E+06	6.38E+06	6.87E+06	5.74E+06	6.29E+06	5.68E+06	4.03E+06
		-25.2	-19.6	-14	-8.4	-2.8	2.8	8.4	14	19.6	25.2
		A	B	C	D	E	F	G	H	I	J

Over	1.05E+07
9.00E+06	1.05E+07
8.50E+06	9.00E+06
7.00E+06	8.50E+06
5.50E+06	7.00E+06
5.00E+06	5.50E+06
Less Than	5.00E+06

Relative Error

Maximum – 12.2%
Average – 8.1%

Figure 4. 65:1 Aperture – Total Neutron Flux (n/cm^2* sec) Calculated from MCNP Mesh Tally.

1	25.2	2.64E+06	3.31E+06	3.19E+06	4.02E+06	4.99E+06	4.16E+06	3.83E+06	3.94E+06	3.63E+06	3.80E+06
2	19.6	3.11E+06	4.23E+06	4.26E+06	4.32E+06	5.52E+06	5.38E+06	5.52E+06	4.98E+06	4.06E+06	4.35E+06
3	14	3.53E+06	3.42E+06	4.05E+06	5.28E+06	4.57E+06	5.48E+06	5.43E+06	5.37E+06	4.07E+06	4.32E+06
4	8.4	3.62E+06	3.21E+06	5.23E+06	4.73E+06	5.19E+06	4.89E+06	5.71E+06	5.08E+06	5.93E+06	6.19E+06
5	2.8	4.31E+06	3.46E+06	5.07E+06	5.62E+06	7.65E+06	5.81E+06	5.05E+06	5.92E+06	5.99E+06	5.21E+06
6	-2.8	3.27E+06	5.21E+06	4.92E+06	4.91E+06	6.49E+06	5.69E+06	6.79E+06	5.80E+06	6.09E+06	4.61E+06
7	-8.4	2.93E+06	4.04E+06	4.84E+06	5.12E+06	5.91E+06	5.54E+06	4.95E+06	5.64E+06	5.82E+06	4.85E+06
8	-14	2.75E+06	3.76E+06	4.16E+06	4.23E+06	5.19E+06	4.67E+06	6.34E+06	5.00E+06	4.63E+06	4.43E+06
9	-19.6	3.06E+06	4.28E+06	4.00E+06	4.24E+06	5.10E+06	4.88E+06	4.59E+06	4.40E+06	4.43E+06	4.52E+06
10	-25.2	1.91E+06	3.53E+06	3.98E+06	4.31E+06	4.38E+06	3.65E+06	3.98E+06	3.78E+06	3.87E+06	3.15E+06
		-25.2	-19.6	-14	-8.4	-2.8	2.8	8.4	14	19.6	25.2
		A	B	C	D	E	F	G	H	I	J

Over	5.80E+06
5.30E+06	5.80E+06
4.80E+06	5.30E+06
4.40E+06	4.80E+06
4.00E+06	4.40E+06
3.40E+06	4.00E+06
Less Than	3.40E+06

Relative Error

Maximum – 14.1%
Average – 10.3%

Figure 5. 125:1 Aperture – Total Neutron Flux (n/cm^2* sec) Calculated from MCNP Mesh Tally.

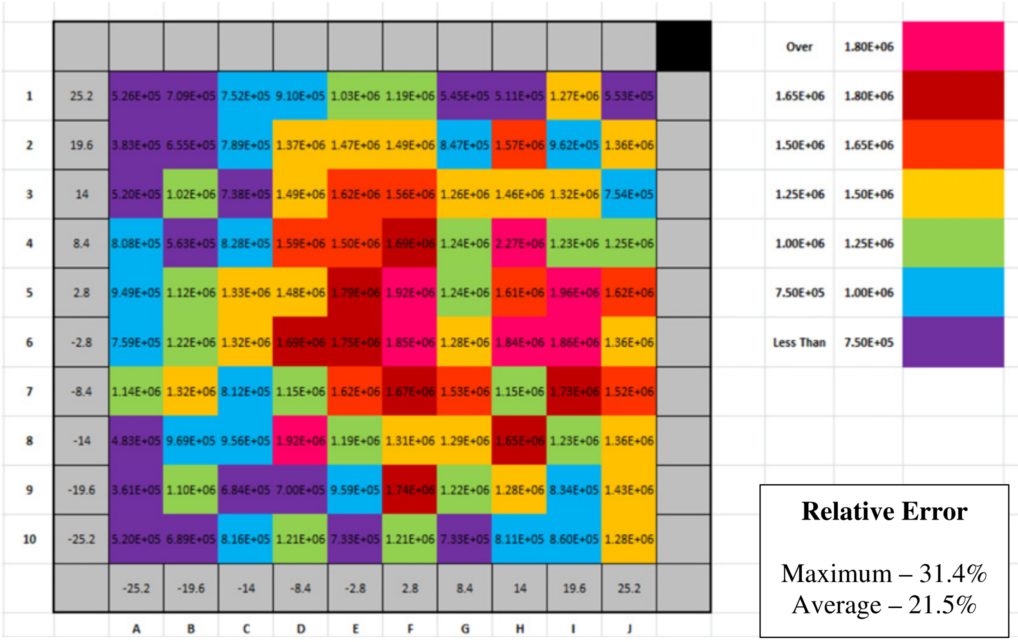

Figure 6. 250:1 Aperture – Total Neutron Flux (n/cm^2* sec) Calculated from MCNP Mesh Tally.

Table 2. Physical Data Associated with Dosimetry.

	Dysprosium	Indium	Units
Foil Dimension	$1 \times 1 \times 0.004$	$1 \times 1 \times 0.004$	inches
Average cross section	1863	4277	barns
Half life	8388	3252	sec
Decay Constant	8.26E–05	2.13E–04	sec^{-1}
Molar Mass	162.500	114.818	g/mol
Activation Energy	0.006–0.065	0.09–2	eV
Mass Fraction, In-115		0.9578	
Branching Ratio, 1293 keV γ		0.844	
Avogadro's Number		6.02E+23	atom/mol

All dosimetry were natural In and Dy samples, Table 2 lists the physical characteristics of the dosimetry used for these calculation based on the Chart of the Nuclides 16$^{\text{th}}$ Edition [6]. The cross sections for each isotope were calculated by averaging the ENDF/B-VII cross sections from 0.006 eV to 2 eV. No weights were applied to energy bins. These energy bins correspond to the energy range at the imaging plane of the radiography facility based on modeled values and confirmed using neutron spectroscopy.

The dosimetry was arranged above the imaging plane in clusters such that the calculated flux in each location would be indicative of the energy dependence of the flux.

2.3 Gamma and Neutron Dose Rate

CaF TLDs were used to quantify the gamma dose at the imaging plane. An Eberline NRD “remball” was also used to quantify dose to tissue at the imaging plane. The collected tissue dose will be useful for

Table 3. CaF and Remball Dose Rate at 90% Reactor Power at Center of Imaging Plane.

Aperture	CaF Dose [Rad/Hr]	Remball Dose [rem/Hr]
65:1	20.6	25.4
125:1	8.2	11.2
250:1	3.4	4.0

planning operations in which experimental scientists and staff may be in close proximity to the neutron radiography tube during operations. The results are in Table 3.

The remball was set to over-range at 5 rem/hr and is calibrated to a bare Pu-Be source. This is a Sandia National Laboratories count lab specific setting and calibration. Based upon the MCNP results and foil data the dominant neutron energy is thermal; therefore, additional spectral calculations were not performed. To estimate the neutron flux at 90% reactor power, measurements were made at lower power levels (0.05, 0.1, 0.2, 0.5, 1.0, 5.0, and 10.0%) and then a linear fit was used to extrapolate the anticipated reading at 90% reactor power. The remball provides a dose output, therefore a neutron conversion factor (3.67E-6 Rem/hr/n/cm^2 s) [7] from flux to dose over the thermal range was used to estimate the neutron flux.

2.4 Neutron Flux Model Validation with Dosimetry Results

The MCNP mesh tally grid was based on an even 10×10 subdivision of the void area within the radiography tube in the model, which resulted in squares approximately 5.6 cm per side. The dosimetry was placed over the radiography tube for irradiation on a 25×25 grid, with squares 2.54 cm per side. In order to correlate the data, the grids corresponding to the MCNP tally and the dosimetry layout were superimposed with the weighted MCNP mesh grid to correspond to the location of the dosimetry, for comparison purposes. The 125:1 aperture only used 12 foils not 13. Note that due to slight differences in dosimetry location, the MCNP weighted values differ for In and Dy. The results are displayed in Table 4.

Table 5 provides a summary of the average of In and Dy foils, MCNP full energy spectrum, MCNP spectrum at foil specific energy ranges, and the estimated flux from the remball at the center of the imaging plane. The spatial average of the foils was used to compare with an energy binned flux tally taken over the entire area of the imaging plane, the total of all bins is shown as "Foil Range MCNP". Experiment packages range in size from a few square centimeters to the entire area of the imaging plane. A gradient is present over the entire imaging plane; however, the average foil result may prove to be relevant for certain large experiments.

The reactor power of 90% was selected to ensure an appropriate balance of irradiation time, decay half-lives, and activation for counting the dosimetry. The time delay between reactor shutdown and processing the dosimetry was approximately one hour.

3. Conclusions

The neutron spectrum at the imaging plane is a thermal spectrum as anticipated, based on the MCNP model and confirmed through activation foils and neutron MicroSpec. The MCNP calculated flux is within approximately 50 percent of the activation foils. At this time we do not have neutron instrumentation capable of measuring the spectrum without over-ranging at extremely low reactor powers to quantify the fast spectrum which may exist. Activation foils that have a large cross section for fast neutrons did not activate sufficiently to count the foils. The modeled spatial tallies indicate a shift which is not apparent in the actual dosimetry, indicating a possible discontinuity in the model.

Table 4. MCNP to Dosimetry Flux Comparisons (n/cm2* sec).

	Foil #	MCNP Weighted Flux (In)	In Flux Results	% Diff Foil/MCNP	MCNP Weighted Flux (Dy)	Dy Flux Results	% Diff Foil/MCNP
65:1	1	8.00E+06	2.76E+06	189.86%	8.63E+06	6.49E+06	32.91%
	2	4.82E+06	1.93E+06	149.47%	4.82E+06	4.56E+06	5.63%
	3	1.07E+07	3.18E+06	235.65%	8.40E+06	7.39E+06	13.70%
	4	8.75E+06	1.46E+06	498.12%	8.75E+06	7.76E+06	12.71%
	5	9.63E+06	6.87E+06	40.16%	9.88E+06	6.44E+06	53.43%
	6	1.06E+07	8.78E+06	20.50%	1.03E+07	7.77E+06	33.24%
	7	7.41E+06	7.33E+06	1.09%	7.53E+06	6.45E+06	16.80%
	8	8.20E+06	7.47E+06	9.83%	9.68E+06	7.06E+06	37.13%
	9	8.14E+06	9.01E+06	9.66%	8.14E+06	6.84E+06	19.01%
	10	4.03E+06	3.98E+06	1.29%	4.04E+06	2.81E+06	43.98%
	11	6.63E+06	6.99E+06	5.10%	6.41E+06	4.91E+06	30.46%
	12	3.79E+06	4.80E+06	20.94%	4.04E+06	2.86E+06	41.05%
	13	6.51E+06	9.08E+06	28.25%	7.74E+06	5.52E+06	40.23%
	Average	**7.48E+06**	**5.66E+06**	**93.07%**	**7.57E+06**	**5.91E+06**	**29.25%**
125:1	14	5.10E+06	4.15E+06	22.88%	5.48E+06	6.12E+06	10.50%
	15	3.84E+06	3.57E+06	7.37%	3.84E+06	5.00E+06	23.32%
	16	5.08E+06	4.20E+06	21.10%	5.37E+06	6.21E+06	13.59%
	17	5.00E+06	4.15E+06	20.51%	5.00E+06	5.99E+06	16.43%
	18	5.45E+06	4.61E+06	18.23%	5.38E+06	5.65E+06	4.74%
	19	6.09E+06	4.75E+06	28.32%	6.41E+06	5.81E+06	10.31%
	20	4.88E+06	4.71E+06	3.53%	4.99E+06	5.69E+06	12.22%
	21	4.05E+06	4.48E+06	9.61%	5.23E+06	5.53E+06	5.52%
	22	4.16E+06	5.25E+06	20.70%	4.16E+06	5.70E+06	26.93%
	23	2.80E+06	3.45E+06	18.93%	2.87E+06	3.39E+06	15.38%
	24	4.06E+06	4.80E+06	15.36%	3.92E+06	5.01E+06	21.77%
	25	2.45E+06	3.93E+06	37.69%	2.49E+06	3.89E+06	36.15%
	Average	**4.41E+06**	**4.34E+06**	**18.69%**	**4.59E+06**	**5.33E+06**	**16.40%**
250:1	1	1.53E+06	6.12E+05	149.22%	1.70E+06	2.29E+06	25.60%
	2	1.35E+06	6.08E+05	122.50%	1.35E+06	2.28E+06	40.67%
	3	2.27E+06	6.00E+05	277.58%	1.46E+06	2.27E+06	35.47%
	4	1.65E+06	6.67E+05	148.06%	1.65E+06	2.24E+06	26.03%
	5	1.48E+06	7.46E+05	99.01%	1.49E+06	2.21E+06	32.43%
	6	1.80E+06	7.51E+05	139.81%	1.83E+06	2.11E+06	13.38%
	7	1.74E+06	7.47E+05	132.36%	1.35E+06	2.09E+06	35.56%
	8	7.38E+05	7.19E+05	2.64%	8.28E+05	2.10E+06	60.54%
	9	9.56E+05	8.28E+05	15.52%	9.56E+05	2.13E+06	55.08%
	10	4.78E+05	8.57E+05	44.16%	5.87E+05	1.85E+06	68.26%
	11	1.01E+06	8.98E+05	12.87%	9.14E+05	2.07E+06	55.92%
	12	5.76E+05	8.48E+05	32.04%	4.41E+05	2.01E+06	78.07%
	13	1.17E+06	1.06E+06	9.84%	1.23E+06	2.18E+06	43.56%
	Average	**1.29E+06**	**7.65E+05**	**91.20%**	**1.22E+06**	**2.14E+06**	**43.89%**

Table 5. Comparison of Variously Calculated Flux.

	Flux [n/cm^2 s]					
Aperture	**Dy Foil**	**Dy Range MCNP+**	**In Foil**	**In Range MCNP +**	**Remball***	**Full Range MCNP**
65:1	5.91E+06 ± 1.51E+05	4.90E+06 ± 5.34E+04	5.66E+06 ± 1.33E+04	7.21E+06 ± 6.56E+04	1.28E+07 ± 1.28E+06	8.24E+06 ± 7.16E+4
125:1	5.33E+06 ± 1.37E+05	2.84E+06 ± 4.03E+04	4.34E+06 ± 1.24E+04	4.25E+06 ± 5.06E+04	5.07E+06 ± 5.07E+05	4.80E+06 ± 5.57E+4
250:1	2.14E+06 ± 4.83+04	7.53E+05 ± 2.21E+04	7.65E+05 ± 4.75E+03	1.11E+06 ± 2.69E+04	1.45E+06 ± 1.45E+05	1.24E+06 ± 2.93E+04

*Remball is an estimate since this flux value is based upon a dose rate instrument.

+ The specific foil MCNP spectrum is an average over the entire imaging plane. As a result the MCNP values are relatively lower than the center foil results.

4. Future Work

Due to time constraints and reactor availability, only one dosimetry result per location was obtained. Each aperture will be characterized via activation foils a minimum of three times to confirm which aperture has the most repeatable spectrum and is most accurately represented by the model, which will be valuable information for experimenters. In addition, the 500:1 aperture plug will be removed to enable characterization. Final characterization work of the neutron radiography tube will also include the experimental region at the base of the tube. The neutron spectrum at the experimental region is anticipated to include fast neutrons; thus allowing for the use of different activation foils and taking advantage of cadmium cutoff experimentation. This additional dosimetric verification will allow for refinement of the MCNP model so it can be utilized for future experimental predictions.

References

[1] MCNP – A Gen. Monte Carlo N-Part. Trans. Code, V5, LA-UR-03-1987, Los Al., NM (2003)
[2] M. Franco Jr, Health Phys. Tech., Sandia Nat. Lab. New Mexico, USA
[3] L.M.R Snoj, Calc. of Pow. Dens. with MCNP in TRIGA reac, Int. Conf. Nuc. En. for New Eur. (2006)
[4] D. Vehar, Nuc. Eng., Sandia Nat. Lab., New Mexico, USA
[5] J.J. Bevelacqua. Basic Health Physics:2nd Edition. WILEY-VCH (2010)
[6] E. Baum, H Knox, T. Miller, Nucl. and Iso. Chart of the Nuclides. 16th Ed. **54,60** (2002)
[7] S.G. Kwon, Calc. Neut. and G-Ray Flux-to-Dose-Rate Conv. Fac, Korea At. En. Res. Inst. (1980)